



ELSEVIER

Contents lists available at ScienceDirect

Biosensors and Bioelectronics

journal homepage: www.elsevier.com/locate/bios

Short communication

A droplet-based microfluidic immunosensor for high efficiency melamine analysis

Jae-Won Choi^{a,1}, Kyong-Mi Min^{a,1}, Sundar Hengoju^a, Gil-Jung Kim^a, Soo-Ik Chang^{a,2}, Andrew J. deMello^b, Jaebum Choo^{c,*}, Hak Yong Kim^{a,*}^a Department of Biochemistry, Chungbuk National University, Cheongju 28644, Republic of Korea^b Department of Chemistry & Applied Biosciences, ETH Zürich, Vladimir Prelog Weg 1, 8093 Zürich, Switzerland^c Department of Bionano Technology, Hanyang University, Ansan 15588, Republic of Korea

ARTICLE INFO

Article history:

Received 9 November 2015

Received in revised form

9 December 2015

Accepted 12 December 2015

Available online 15 December 2015

Keywords:

Melamine

Droplet-based microfluidics

Fluorescence polarization

Milk

ABSTRACT

We report a droplet-based microfluidic immunosensor for the rapid and accurate detection of melamine, an organic base that has been implicated in widescale adulteration of food products such as milk. Our melamine assay is based on the competitive reaction between native melamine and a melamine-fluorescein isothiocyanate (FITC) conjugate against an anti-hapten antibody. The adoption of fluorescence polarization, allows the quantification of melamine in a more direct and rapid manner than established heterogeneous methods based on liquid chromatography, mass spectrometry, and enzyme-linked immunosorbent assay (ELISA). The detection protocol provides a limit of detection of 300 ppb, which is below the maximum allowable melamine levels (2.5 ppm) defined by the U.S. Food and Drug Administration and the European Commission to a significant extent.

© 2016 Elsevier B.V. All rights reserved.

1. Introduction

Melamine (1,3,5-triazine-2,4,6-triamine) is a nitrogen-rich heterocyclic triazine used to produce a range of products including plastics, laminates, coating agents, foams, pigments, glues and fire-retardants (Tyan et al., 2009; Ellis et al., 2012). Melamine is commonly but illegally added to food products (such as dairy products and animal feeds) to increase the apparent protein content, due to its low cost and high nitrogen content. Illegally added melamine in food products can cause significant health effects to the consumer, including blindness, kidney stones, reproductive damage and cancer (Duan et al., 2015). For example, the discovery of severe kidney damage to children and pets initiated widespread milk and pet food recalls in the USA and China in 2007 and 2008 (Li et al., 2015). A consequence of such incidents has been the limitation of melamine in food products to concentrations below 2.5 ppm by the U.S. Food and Drug Administration (FDA), the European Commission, and other countries (Dai et al., 2014; Du et al., 2015; Fashi et al., 2015). Despite tighter regulations, reports of food products containing melamine at elevated levels are still common (Li et al., 2015). Accordingly, the need for a sensitive, robust and

universal method to detect melamine in food products is apparent.

Various methods of detecting melamine have been introduced in recent years. These include the use of liquid chromatography–mass spectrometry (LC–MS) (Feng et al., 2008), gas chromatography–mass spectrometry (GC–MS) (Squadrone et al., 2010), high performance liquid chromatography (HPLC) (Zhou et al., 2010), chip-based ion mobility spectrometry (Zhao et al., 2015), electrochemical sensing (Liu et al., 2015), surface enhanced Raman scattering (SERS) (Guo et al., 2014; Li et al., 2015), enzyme-linked immunosorbent assays (Lei et al., 2010) and surface plasmon resonance (SPR) (Qi et al., 2010). Although many of these exhibit excellent sensitivity and limits of detection, almost all involve a variety of pre-processing and multiple reaction steps, which limit their analytical speed. More recently, a number of studies have addressed such limitations, with a view to performing rapid melamine analysis using chemiluminescence resonance energy transfer (Du et al., 2015), fluorescence resonance energy transfer (Wu et al., 2015), colorimetric assays (Kumar et al., 2014) and molecularly imprinted polymer (Liu et al., 2015; Xu and Lu, 2015). These methods have been highly successful in reducing assay times, but are somewhat compromised due to high limits of detection and synthesis of additional particles (or polymers).

To this end, we propose the use of fluorescence polarization (FP) to provide for the rapid and sensitive detection of melamine in real-world samples. Since FP-based methods are homogeneous in nature, they do not require additional pre-processing steps, the use of extrinsic reporter species or the separation of bound and

* Corresponding authors.

E-mail addresses: jwchoi21@chungbuk.ac.kr (J.-W. Choi),jbchoo@hanyang.ac.kr (J. Choo), hykim@chungbuk.ac.kr (H.Y. Kim).¹ Contributed equally to this work.² Deceased.

free species from the analytical sample to allow analysis. (Checovich et al., 1995; Choi et al., 2015). Specifically, we present a fluorescence polarization immunoassay integrated with droplet-based microfluidic sample processing to detect melamine in sub-nanoliter volumes. Droplet-based (or segmented-flow) microfluidic systems have emerged as an effective instrumental platform for performing high-throughput chemical and biological experiments. Put simply, picoliter-volume droplets (or plugs) may be generated rapidly (kHz–MHz rates), with their size and biological payloads being controlled in a reproducible manner. In principle, each droplet acts as an individual compartment that isolates and protects its contents from the external environment. Unsurprisingly, droplet-based microfluidic systems have been successful in performing a range high-throughput assays (Guo et al., 2012; Niu et al., 2011; Theberge et al., 2010; Zhu and Fang, 2013). In a recent study, we introduced the use of fluorescence polarization to probe protein–protein interactions in a high-throughput manner (Choi et al., 2012). Specifically, the interaction between angiogenin and anti-angiogenin antibody and the efficient extraction of dissociation constants could be achieved with high precision and within short time periods. In a similar manner, we herein combine fluorescence polarization and droplet-based microfluidics for rapid and sensitive detection of melamine in food samples. Furthermore, our proposed fluorescence polarization-based microdroplet sensor allows a cost-effective detection of melamine because the amounts of expensive antibodies and fluorophores are dramatically reduced.

2. Experimental

2.1. Materials

Melamine (M.W. 126.12 g/mol), fluorescein isothiocyanate isomer-I (FITC), N,N-dimethylformamide (DMF), trimethylamine for fluorescent conjugation were purchased from Sigma-Aldrich (St. Louis, MO, USA). Phosphate buffered saline (PBS) was purchased from Amresco (Solon, OH, USA) and 1-ethyl-3-(3-dimethylaminopropyl) carbodiimide hydrochloride (EDC) was purchased from Life Technologies (Carlsbad, CA, USA). Hapten (3-((4,6-diamino-1,3,5-triazin-2-yl)thio)propanoic acid) and anti-hapten antibody were obtained from 21st Century Biochemicals (Marlborough, MA, USA) and bovine serum albumin (BSA) was purchased from GenDEPOT (Barker, TX, USA). Sylgard 184 elastomer base and curing agent were purchased from Dow Corning (Midland, MI, USA). Abil EM 90 surfactant was purchased from Evonik Industries (Essen, Germany) and mineral oil was purchased from Sigma-Aldrich (St. Louis, MO, USA). All chemicals were used as received.

2.2. Antibody production

A suitable hapten was used as an immunogen for efficient melamine detection. The structure of hapten is similar to melamine as shown in supporting information (Fig. S1). Hapten was conjugated to BSA using EDC and the resulting conjugate was used for immunization in a rabbit. Collected sera from the rabbit were purified and prepared for detection of melamine using standard protocols (Lei et al., 2010).

2.3. Western blot analysis

Each prepared sample (hapten-BSA and BSA) was mixed with protein sample buffer, heated at 100 °C for 5 min, subjected to SDS-PAGE, and subsequently transferred onto a polyvinylidene fluoride membrane. The membrane was then blocked with 5% skimmed milk in PBS containing Tween 20 for 1 h and incubated

with anti-hapten antibody and HRP-conjugated secondary antibody at room temperature. Following extensive washing, reactive bands were visualized using enhanced chemiluminescence (ECL) western blotting detection reagents (WEST-ZOL Plus) from iNtRON Biotechnology (Seongnam, Republic of Korea). Images were captured using Ez-Capture ATTO imaging system (AE-9100N, Tokyo, Japan).

2.4. Preparation of melamine-FITC conjugate

0.1 mg of melamine was dissolved in 10 μ L of DMF, and then 1 μ L triethylamine and 0.1 mg FITC was added and completely mixed. The solution was then incubated overnight at room temperature. After conjugation, the solution was spotted onto a thin layer chromatography (TLC) silica gel glass plate (Merck Millipore, Billerica, MA, USA). The plate was loaded into a TLC vessel and eluted with chloroform and methanol solvent mixture (4:0.4, v/v). The main yellow band at $R_f=0.5$ was removed and extracted in methanol by overnight incubation at 4 °C. Silica was removed from the extracted fraction by centrifugation at 4 °C, 7000 rpm, for 20 min. The concentration of the purified melamine-FITC conjugate was determined using a NanoDrop 2000 UV-vis spectrophotometer from Thermo Fisher Scientific (Waltham, MA, USA).

2.5. Microfluidic device fabrication

The PDMS device was fabricated using standard soft lithographic techniques (Bardiya et al., 2014; Chung et al., 2013; DiCicco and Neethirajan, 2014). Briefly, the elastomer base and curing agent were mixed in a weight ratio of 10:1 and poured onto a patterned Si-wafer mask. After curing on a heating plate at 75 °C for 3 h, the cured PDMS block was peeled off and holes were punched using a 1.0 mm diameter disposable biopsy punch. After treatment in an oxygen plasma, the structured PDMS layer and glass slide were bonded immediately and cured on a heating plate.

2.6. Droplet-based fluorescence polarization (DFP) assay

A microfluidic device containing 3-aqueous inlets was used in for experiments. Abil EM 90 of 2% (w/w) in mineral oil was used as the continuous carrier fluid. The microfluidic device was operated using volumetric flow rates 0.5 μ L/min for each aqueous inlet and 1.0 μ L/min for the oil inlet using precision syringe pumps (PHD 2000, Harvard Apparatus, Holliston, MA, USA). FP originating from the generated microdroplets was measured using fluorescence microscopy. The system consisted of a 10 mW, 488 nm diode laser (World Star Tech, Toronto, ON, Canada), an inverted fluorescence microscope (Olympus IX71, Tokyo, Japan), and a dual fluorescence polarization detection system. An electron multiplying-charge coupled device (ProEM, Princeton Instruments, Trenton, NJ, USA) was used for the detection of polarized emission.

2.7. Conventional fluorescence polarization assay

A conventional FP assay was performed using a Beacon 2000 Fluorescence Polarization System from Life Technologies (Carlsbad, CA, USA). The volume of each sample was 200 μ L and FP measurements were performed at room temperature.

3. Results and discussion

3.1. Characterization of anti-hapten antibody with melamine

Melamine has three amino groups on the triazine ring having the same reactivity. As to this structure, it hinders efficient

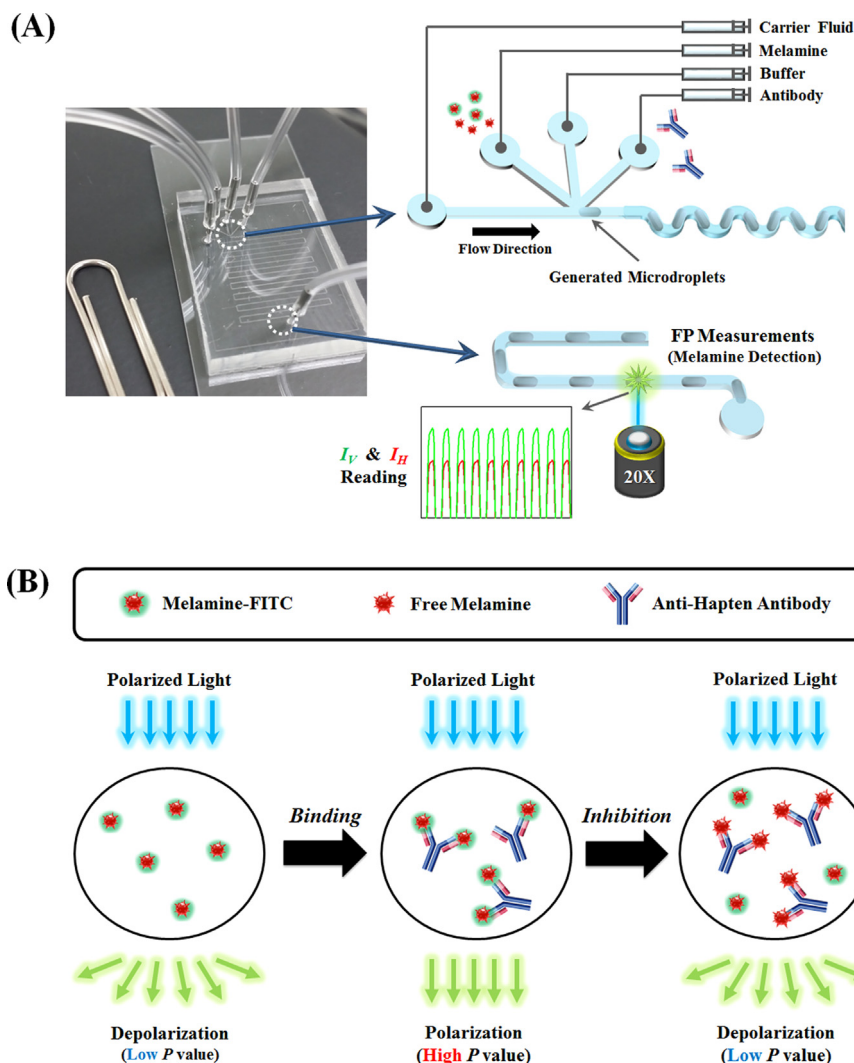


Fig. 1. Schematic illustration of the droplet-based immunosensor for melamine detection. (A) Three aqueous inlets (T-junction) chip was used for droplet generation. Melamine (free melamine and melamine-FITC conjugate), buffer (phosphate buffered saline, pH 7.4), and anti-hapten antibody were injected through left, middle, and right inlets, respectively. Fluorescence polarization (FP) from each droplet was measured through 20 \times objective at the end of the channel of microfluidic chip. Vertical intensity (I_V) and horizontal intensity (I_H) were measured simultaneously. (B) Schematic of the concept behind fluorescence polarization of the binding between melamine-FITC and antibody, and the competitive inhibition between melamine-FITC and antibody using free melamine. The interaction between melamine-FITC and anti-hapten antibody will give higher fluorescence polarization (P) value than of the only melamine-FITC. The P value of melamine-FITC/anti-hapten antibody will decrease when melamine-FITC is replaced by free melamine.

production of anti-melamine antibody. Accordingly, a structurally related compound, hapten (3-((4,6-diamino-1,3,5-triazin-2-yl)thio)propanoic acid), served as an immunogen (Fig. S1). Hapten needs a carrier protein to take part in immune reactions, and thus bovine serum albumin (BSA) was used as a carrier. It should be noted that there have been previous reports detailing successful melamine detection using the anti-hapten antibody (Cao et al., 2013; Lei et al., 2010; Yin et al., 2010).

Firstly, western blot analysis was conducted on both the hapten-BSA conjugate and BSA to see if anti-hapten antibodies combine only with hapten. Fig. S2, clearly demonstrates that the anti-hapten antibodies uniquely interact with hapten, with no non-specific binding with BSA being observed. Melamine was then conjugated with FITC to confirm by FP if the antibodies in the previous step can bind with melamine. The melamine-FITC conjugate was purified using thin layer chromatography as shown in Fig. S3.

As noted, the binding between melamine and anti-hapten antibody was then probed using the droplet-based microfluidic system described in Fig. 1. Melamine-FITC, PBS, and anti-hapten

antibody were injected via the left inlet, the middle inlet, and the right inlet, respectively, with mineral oil containing 2% (w/w) Abil EM 90 serving as the carrier fluid for droplet isolation. The final concentration of the melamine-FITC conjugate was fixed at 0.5 nM and the antibody concentration varied between 0 and 500 nM. The extracted polarization value (P) from each concentration of anti-hapten antibody was calculated using Perrin's equation (Checovich et al., 1995) and normalized using Eq. (1):

$$y = \frac{(P_{max} - P_x)}{(P_{max} - P_{min})} \quad (1)$$

Here P_{max} and P_{min} represent maximal and minimal P values, respectively. P_x represents the P value at each concentration (x) of anti-hapten antibody. As the concentration of anti-hapten antibody increases, P values increase until saturation. In these droplets, the rotational diffusion can be significantly hindered if the melamine-FITC binds to an anti-hapten antibody (larger molecule). The droplet-based microfluidic system was then used to quantify the binding affinity of melamine against anti-hapten antibody. The extracted value of 124.0 ± 10.9 nM for the

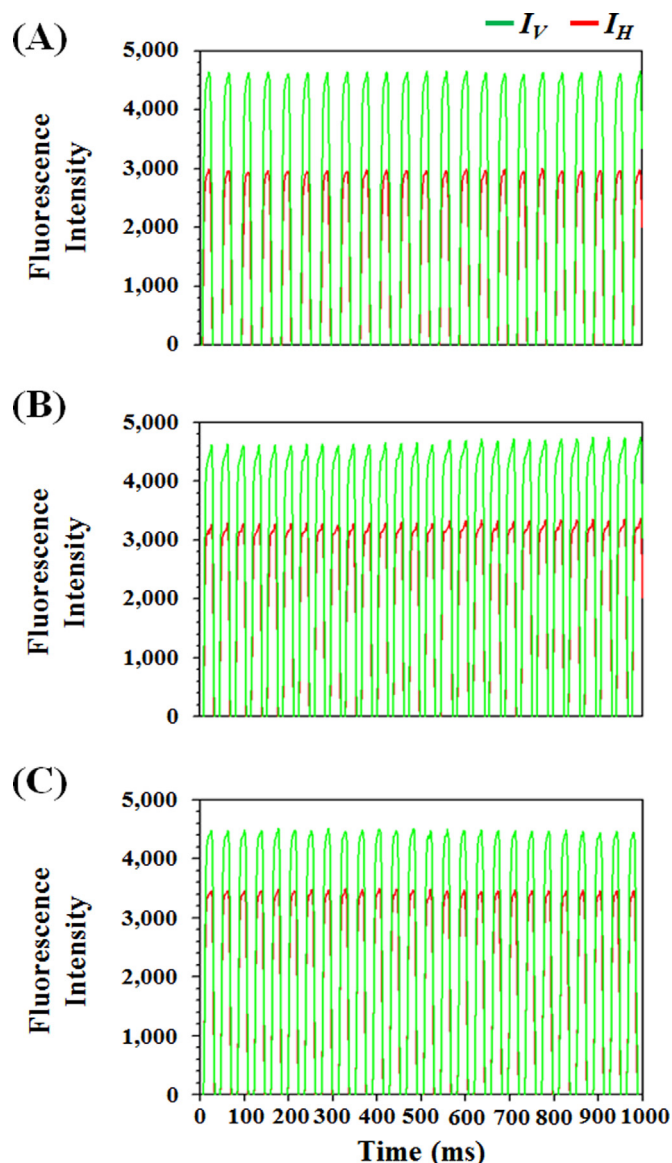


Fig. 2. Exemplar fluorescence burst scans recorded over a time period of 1 s. The concentration of the melamine-FITC and anti-hapten antibody was fixed at 0.5 nM and 120 nM, respectively, and the concentration of free melamine was titrated (A) 0.06, (B) 3.9, and (C) 25.0 $\mu\text{g mL}^{-1}$. Green lines and red lines represent vertical intensity (I_V) and horizontal intensity (I_H), respectively. (For interpretation of the references to color in this figure legend, the reader is referred to the web version of this article.)

dissociation constant is in close agreement with results obtained from conventional FP assay (120.0 ± 8.5 nM) required 200 μL volume per each sample as shown in Fig. S4.

3.2. Calibration curve for melamine detection in microdroplets

A competitive inhibition assay for anti-hapten antibody using free melamine and melamine-FITC was performed to detect melamine, and the data used to generate a calibration curve. The 3-inlet microfluidic device was again also used. Specifically, the free melamine and the melamine-FITC mixture, PBS, and the anti-hapten antibody were injected into the left, middle, and right inlets, respectively. The concentrations of melamine-FITC and anti-hapten antibody in the competitive inhibition assay were fixed at 0.5 nM and 120 nM, respectively, and the concentration of free melamine was titrated between 0.01 and 100 $\mu\text{g mL}^{-1}$. An example of typical vertical intensity (I_V) and horizontal intensity (I_H)

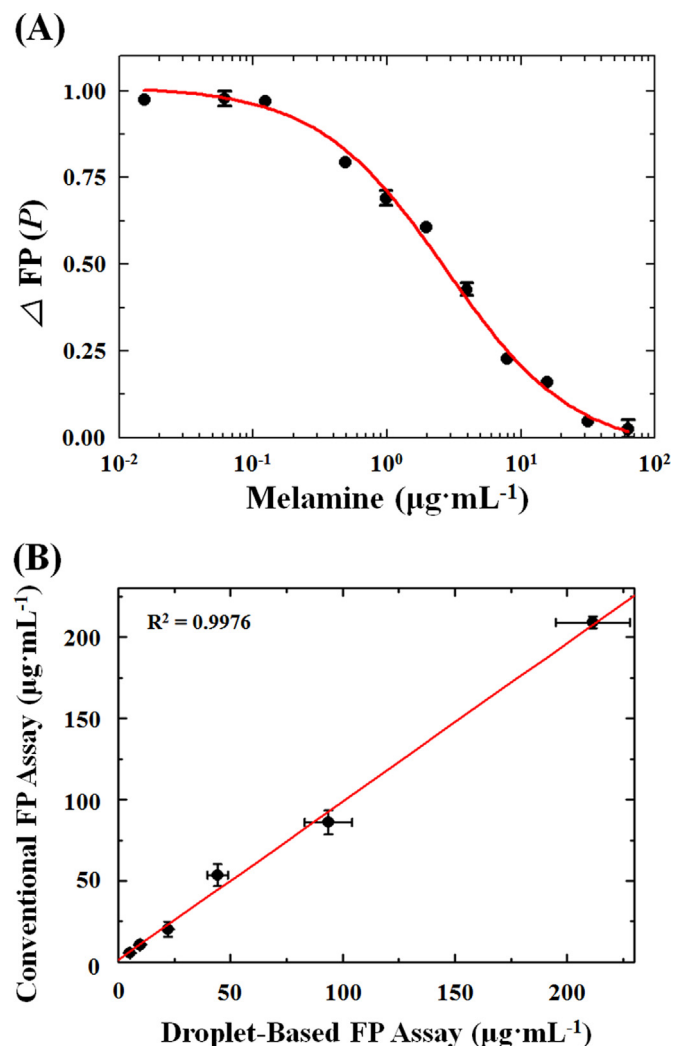


Fig. 3. (A) Titration curve for melamine detection using droplet-based FP assay. Competitive inhibition assay for titration between free-melamine and melamine-FITC conjugate against anti-hapten antibody was performed. The IC_{50} value was 3.0 ± 0.2 $\mu\text{g mL}^{-1}$. (B) Correlation analysis of droplet-based FP assay and conventional FP assay for melamine detection in milk sample. Melamine was spiked in milk with the concentration of 5, 10, 20, 50, 100, and 200 $\mu\text{g mL}^{-1}$. The R^2 value was 0.9976.

of the emitted light from droplets burst scans over a time period of 1 s are presented in Fig. 2. Although vertical intensities have a similar values, it is observed that variations of horizontal intensities from each sample.

The extracted polarization values for each free melamine concentration was processed using Eq. (1), and the final titration curve was obtained using Eq. (2)

$$y = \frac{(P_{\max} - P_{\min})}{\left[1 + \left(\frac{x}{IC_{50}}\right)^S\right]} + P_{\min} \quad (2)$$

P_{\max} and P_{\min} define the maximal and minimal P values, S corresponds to the slope of the sigmoidal curve, and IC_{50} defines the melamine concentration at 50% of tracer binding. As the concentration of free-melamine increases, the P values were reduced since free-melamine act as competitor of melamine-FITC.

For melamine concentrations between 0.71 and 12.73 $\mu\text{g mL}^{-1}$ inhibition efficiencies between 20% and 80% are obtained from the titration curve, and the limit of detection is calculated to be 0.30 $\mu\text{g mL}^{-1}$ (Fig. 3A). These results show that detection is possible with a limit of detection more than 8-times lower than 2.5 ppm

standard defined by the U.S. FDA and European Commission. Critically, the parameters extracted using the droplet-based microfluidic system are in excellent agreement with the parameters obtained from conventional spectrophotometer (Table S1), whilst consuming over five orders of magnitude less sample (about 1 nL) than conventional assay (200 μL) and spending two orders of magnitude less analytical time (50 ms per sample) than conventional assay (over 10 s per sample). This indicates that the assay cost can be reduced over five orders of magnitude because only small amounts of fluorophores and antibodies are needed for melamine analysis.

3.3. Application to real sample analysis

To extend our experimental approach for the practical use, we have investigated the quantitation of melamine in milk. Various concentrations of melamine (between 5 and 200 $\mu\text{g mL}^{-1}$) were artificially added into raw milk samples to assess the applicability of the method to real world samples. Milk samples containing different concentrations of melamine were used to generate a calibration curve, with all experimental conditions being identical to the previous experiment. Specifically, the milk sample and the melamine-FITC mixture, PBS, and the anti-hapten antibody were injected into the left, middle, and right inlets, respectively. The concentrations of melamine-FITC and anti-hapten antibody in the competitive inhibition assay were fixed at 0.5 nM and 120 nM, as described above.

P values for each of melamine/milk samples were calculated using Eq. (1), and the real melamine concentrations in the milk were calculated using the titration curve. Table S2 shows the measured concentration and theoretical concentration for all experiments, with an average recovery efficiency of 99.9%. Droplet-based microfluidic experiments agree well with results from conventional FP assay, and additionally exhibit a lower mean coefficient of variation (CV). Importantly, an excellent correlation ($R^2=0.99$) between the measurements using conventional spectrometer and the measurements using droplet-based microfluidics is observed Fig. 3B. Using this approach, the detection and quantitation of melamine from milk using DFP assay was successful.

4. Conclusions

In conclusion, we have successfully developed a droplet-based microfluidic immunosensor for the sensitive and rapid detection of melamine. The combined droplet volumes analyzed for each experiment was less than 1 nL, and droplets were generated at a frequency in excess of 25 Hz. Furthermore, analysis of melamine spiked milk samples, demonstrated that the method is successful in detecting melamine contained in commercial milk products at the required sensitivity. The limit of detection of the developed method was more than 8-times lower than than 2.5 ppm maximum permissible level of melamine in foods, and also less than the 1.0 ppm maximum permissible level of melamine that in infant milk formulas. We demonstrate that the developed method reduces required sample volumes by over 5 orders of magnitude when compared to existing conventional FP, ELISA- and SPR-based approaches. Consequently, assay cost could be dramatically saved by reducing the amounts of expensive antibodies and fluorophores through our proposed fluorescence polarization-based microdroplet sensor.

A significant advantage of the DFP assay in detecting melamine

is the homogeneous property of measurement. This contrasts with heterogeneous property of ELISA- and SPR-based approaches and allows rapid detection of melamine by virtue. Finally, we believe that the method is well-suited to in-the-field measurements, and moreover, can be widely applied as an aptasensor using aptamers or a chemisensor using polymers.

Acknowledgments

All authors acknowledge the inspiring contributions of the late Prof. Soo-ik Chang in initiating this study. This work was supported by National Research Foundation (NRF) grant funded by the Ministry of Science, ICT and Future Planning (MSIP) of Korea through Global Research Laboratory (GRL) Program (Grant number 2009-00426).

Appendix A. Supplementary material

Supplementary data associated with this article can be found in the online version at <http://dx.doi.org/10.1016/j.bios.2015.12.023>.

References

- Bardiya, N., Choi, J.W., Chang, S.I., 2014. *Biochip J.* 8, 15–21.
- Cao, B., Yang, H., Song, J., Chang, H., Li, S., Deng, A., 2013. *Talanta* 116, 173–180.
- Checovich, W.J., Bolger, R.E., Burke, T., 1995. *Nature* 375, 254–256.
- Choi, J.W., Kang, D.K., Park, H., deMello, A.J., Chang, S.I., 2012. *Anal. Chem.* 84, 3849–3854.
- Choi, J.W., Kim, G.J., Lee, S., Kim, J., deMello, A.J., Chang, S.I., 2015. *Biosens. Bioelectron.* 67, 497–502.
- Chung, E., Gao, R., Ko, J., Choi, N., Lim, D.W., Lee, E.K., Chang, S.I., Choo, J., 2013. *Lab Chip* 13, 260–266.
- Dai, H., Shi, Y., Wang, Y., Sun, Y., Hu, J., Ni, P., Li, Z., 2014. *Biosens. Bioelectron.* 53, 76–81.
- DiCicco, M., Neethirajan, S., 2014. *Biochip J.* 8, 282–288.
- Du, J., Wang, Y., Zhang, W., 2015. *Spectrochim. Acta A Mol. Biomol. Spectrosc.* 149, 698–702.
- Duan, X., Dai, X.X., Wang, T., Liu, H.L., Sun, S.C., 2015. *Hum. Reprod.* 30, 1677–1689.
- Ellis, D.I., Brewster, V.L., Dunn, W.B., Allwood, J.W., Golovanov, A.P., Goodacre, R., 2012. *Chem. Soc. Rev.* 41, 5706–5727.
- Fashi, A., Yafitian, M.R., Zamani, A., 2015. *Food Chem.* 188, 92–98.
- Feng, J.W., Cai, Q.R., Liu, X.C., Yu, Y.G., Peng, Y.F., Zhang, Y., 2008. *Mod. Food Sci. Technol.* 24, 1058–1060.
- Guo, M.T., Rotem, A., Heyman, J.A., Weitz, D.A., 2012. *Lab Chip* 12, 2146–2155.
- Guo, Z., Cheng, Z., Li, R., Chen, L., Lv, H., Zhao, B., Choo, J., 2014. *Talanta* 122, 80–84.
- Qi, W.J., Wu, D., Ling, J., Huang, C.Z., 2010. *Chem. Commun.* 46, 4893–4895.
- Kumar, N., Seth, R., Kumar, H., 2014. *Anal. Biochem.* 456, 43–49.
- Lei, H., Shen, Y., Song, L., Yang, J., Chevallier, O.P., Haughey, S.A., Wang, H., Sun, Y., Elliott, C.T., 2010. *Anal. Chim. Acta* 665, 84–90.
- Li, X., Feng, S., Hu, Y., Sheng, W., Zhang, Y., Yuan, S., Zeng, H., Wang, S., Lu, X., 2015. *J. Food Sci.* 80, 1196–1201.
- Liu, B., Xiao, B., Cui, L., Wang, M., 2015. *Mater. Sci. Eng. C Mater. Biol. Appl.* 55, 457–461.
- Niu, X., Gielen, F., Edel, J.B., deMello, A.J., 2011. *Nat. Chem.* 3, 437–442.
- Squadroni, S., Ferro, G.L., Marchis, D., Mauro, C., Palmegiano, P., Amato, G., Genin, E. P., Abete, M.C., 2010. *Food Control* 21, 714–718.
- Theberge, A.B., Courtois, F., Schaerli, Y., Fischlechner, M., Abell, C., Hollfelder, F., Huck, W.T., 2010. *Angew. Chem. Int. Ed. Engl.* 49, 5846–5868.
- Tyan, Y.C., Yang, M.H., Jong, S.B., Wang, C.K., Shiea, J., 2009. *Anal. Bioanal. Chem.* 395, 729–735.
- Wu, Q., Long, Q., Li, H., Zhang, Y., Yao, S., 2015. *Talanta* 136, 47–53.
- Xu, S., Lu, H., 2015. *Biosens. Bioelectron.* 73, 160–166.
- Yin, W., Liu, J., Zhang, T., Li, W., Liu, W., Meng, M., He, F., Wan, Y., Feng, C., Wang, S., Lu, X., Xi, R., 2010. *J. Agric. Food Chem.* 58, 8152–8157.
- Zhao, W.J., Wang, Y., Li, J., Li, L.F., Wang, Q., Han, K., Zhang, Y., Li, X., Li, P., Luo, J., Wang, X., 2015. *Food Chem.* 188, 489–495.
- Zhou, J., Zhao, J., Xue, X., Chen, F., Zhang, J., Li, Y., Wu, L., Chen, L., 2010. *J. Sep. Sci.* 33, 167–173.
- Zhu, Y., Fang, Q., 2013. *Anal. Chim. Acta* 787, 24–35.